Intention-Aware Pedestrian Avoidance

Tirthankar Bandyopadhyay[1], Chong Zhuang Jie[2], David Hsu[3], Marcelo H. Ang Jr.[2], Daniela Rus[4], and Emilio Frazzoli[5]

[1] Future Urban Mobility, Singapore MIT Alliance for Research and Technology
[2] Department of Mechanical Engineering, National University of Singapore,
[3] Department of Computer Science, National University of Singapore,
[4] Computer Science & Artificial Intelligence Laboratory, Massachusetts Institute of Technology
[5] Laboratory for Information and Decision Systems, Massachusetts Institute of Technology

Summary. A critical component of autonomous driving in urban environment is the vehicle's ability to interact safely and intelligently with the human drivers and on-road pedestrians. This requires identifying the human intentions in real time based on a limited observation history and reacting accordingly. In the context of pedestrian avoidance, traditional approaches like proximity based reactive avoidance, or taking the most likely behavior of the pedestrian into account, often fail to generate a safe and successful avoidance strategy. This is mainly because they fail to take into account the human intention and the inherent uncertainty resulting in identifying such intentions from direct observations.

This work formulates the on-road pedestrian avoidance problem as an instance of the *Intention-Aware Motion Planning* (IAMP) problem, where the human intention uncertainty is incorporated in a principled manner into the planning framework. Assuming a set of all possible pedestrian intentions in the environment, IAMPs generate a Mixed Observable Markov Decision Process (MOMDP), (a factored variant of *Partially Obervable Markov Decision Process* (POMDP)) with the human intentions being the *unobserved* variables. Solving the resulting MOMDP generates a robust pedestrian avoidance policy. In spite of the criticism of POMDPs to be computationally intractable in general, we show that with proper state factorization and latest sampling based approaches the policy can be executed online on a real vehicle on road. We demonstrate this by running the algorithm on a real pedestrian crossing in the NUS campus successfully handling the intentions for multiple pedestrians, even when they are jaywalking. In this paper, we present results in simulation to show the improved performance of the proposed approach over existing methods. Additionally, we present results validating experimentally the assumptions made in formulating the intention aware pedestrian avoidance problem.

This work presents a preliminary step towards safer and effective autonomous navigation in urban environments by incorporating the intentions of pedestrians and other drivers on the road.

1 Introduction

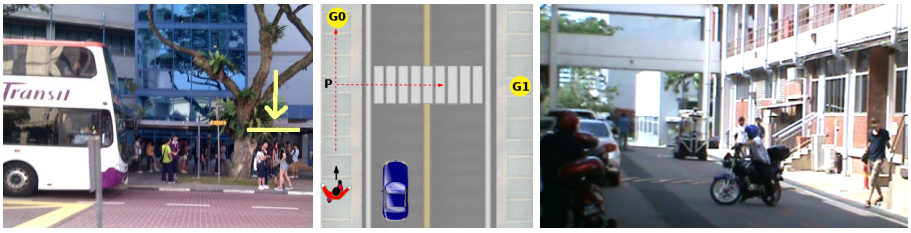

(a) (b) (c)

Fig. 1. Autonomous navigation in a crowded environment requires accounting for the pedestrian intentions.

With robots venturing more into human spaces, it becomes imperative for the robots to predict the motion and intentions of people and other agents in the field for effective operation. A popular example is autonomous vehicles in urban environments which have to react with pedestrians, cyclists and other human drivers on the road. Identifying intentions is even more relevant in the case of autonomous vehicles because in many situations direct communication between the robots and people is not possible, *e.g.*between pedestrians and autonomous vehicles. A popular and simple approach of avoiding pedestrians is that of running a one step prediction interwoven with avoidance based on either potential fields [11], velocity obstacles [7] or by partial motion planning [2] *etc.*at a very high update rate. Due to the reactive approach, the success of such approaches in a crowded environment depends on the assumption that the dynamic nature of the environment will prevent the robot from getting stuck. However this assumption may not hold always. Take the scenario shown in Fig.1(a) of people standing very close to edge of the pedestrian sidewalk. While their position is close to the road, the pedestrian's intentions may not be to actually step on the road. Decisions purely based on the position and not the intention of the pedestrians may cause an autonomous vehicle to get stuck waiting for the pedestrian to cross. Human drivers however make a judgment over the pedestrian's intentions based on their activity (here waiting rather than trying to cross the road) and safely drive on.

Detecting a person's intentions or predicting his/her trajectory has been addressed using Hidden Markov Models [10, 17], non-parametric approaches like Inverse Reinforcement Learning [9], Gaussian Processes [6] and Bayesian Occupancy Filter [4] just to name a few. In most of these approaches the tools have been developed to identify a person's intention as an end goal. Only after the intention has been resolved sufficiently is the robot able to choose its action. In reality, the purpose of the robot is to navigate safely and it should only focus on resolving those pedestrian intentions relevant to

the task. Integrating the intention prediction with motion planning provides a more effective approach. In many cases there might not be enough information for the intention to be completely resolved before the robot has to make a decision. Usually in such cases the robot takes actions against most likely intention [10]. However, not taking into the account the prediction limitation can lead to unsafe actions. Take the case of Fig.1(b) where the pedestrian walking along a sidewalk may move to either G0 or G1 along the marked trajectory. In essence no amount of sensing can effectively predict which goal the pedestrian is moving towards until he/she passes P. A false prediction of G0 due to motion stochasticity or sensing inaccuracy can cause potential collision or evoke emergency avoidance by the robot. In such scenarios it is imperative to not only take the prediction but also take the uncertainty associated with the prediction into the robot's decision process. This work formulates the on-road pedestrian avoidance problem as an instance of the *Intention-Aware Motion Planning* (IAMP) problem presented in [1], where the intention uncertainty is incorporated in a principled manner into the planning framework.

In many cases pedestrian motion models, their desired goals in the environment and their interaction with other entities can be learnt from the data collected by sensors in the environments [6]. We approach the problem assuming that the pedestrian motion models and their possible goals are available. The robot then has to reason about each sensed pedestrian's intention given the short observation history of the pedestrian's motion in making its decision. Even though in general exact solutions to POMDPs are intractable [14], with proper factorization of the observable and unobservable state variables as a Mixed Observable MDP (MOMDP [13]) and sampling based approximate solutions (SARSOP [12]), we show that such an approach can be applied successfully on a real autonomous vehicle in a crowded environment (Fig.1c). Let us now state the problem statement formally:

For a known environment $\mathcal{W}$ and known set of possible pedestrian goal locations Θ in $\mathcal{W}$, find an optimal policy Π, to minimize the time taken for the robot R to reach its goal R_g and avoiding collision in the presence of multiple pedestrians $\boldsymbol{p}_i$ moving towards corresponding goals, $g_i \in \Theta$ where all g_i are unknown to the robot.

2 Technical Approach

The problem of avoiding a single pedestrian $\mathbf{p}_i$ in the environment $\mathcal{W}$, can be described by a few variables, the robot's state: location $\mathbf{x}_r$, velocity $\mathbf{v}_r$, and the pedestrian state: location $\mathbf{x}_i$, his/her intention g_i (here the goal location). In general, $\mathbf{x}_r$, $\mathbf{v}_r$ and $\mathbf{x}_i$ can be estimated from a variety of sensors following an observation function $Z : p(o|\mathbf{x}_r, \mathbf{v}_r, \mathbf{x}_i)$. However under acceptable sensing accuracy we assume them to be fully observed. This helps us reduce the computational complexity of the problem and we show experimentally in Sec.3.2 that

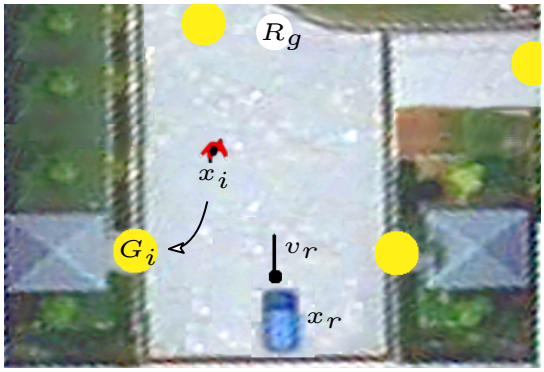

Fig. 2. Pedestrian avoidance scenario in the quadrangle environment shows the relevant variables in the formulation.

this assumption is indeed reasonable. On the other hand, there is no "intention sensor" for g_i and it is treated as unobservable variable. Let $x \in \mathcal{X}$ represent the observed state variables and $g_i \in \mathcal{Y}$ denote the unobserved pedestrian's intention. The robot can pick actions $a \in A : \{cruise, accelerate, deccelerate\}$, to control the vehicle. The choice of using such high level acceleration commands as compared to direct velocity commands mimics human driver behavior who control the brakes and acceleration rather than reason about the actual velocities. The robot is rewarded by a function R when it successfully navigates to its desired goal and is penalized for time delay and collision.

We formulate the pedestrian avoidance problem in autonomous navigation by a discrete MOMDP: $\mathcal{M}_i : (\mathcal{X}, \mathcal{Y}, A, O, Z, T_X, T_Y, R, \gamma)$, where O is the set of all possible observations and γ the discount factor. The transition function $T_X(x, g_i, a, x') : p(x'|x, g_i, a)$ gives the transition of the observed variables from the current observed state x into the future observed state x' upon taking the action a in the state (x, g_i). This incorporates the pedestrian and the robots motion models.

We assume the motion of the pedestrian to follow a trajectory towards its intended goal in a shortest possible path, a simplified model of social potential fields [8]. Note that the pedestrian may not follow the exact shortest path due to personal preferences, distracted walking, avoidance of other pedestrians and vehicles on the road. These unknown variations are modeled with the uncertainty distribution over the intended direction.

$$\mathbf{p}_i{}' = \mathbf{p}_i + v_p \Delta t \hat{\mathbf{n}}_\mathbf{i}$$

where $\hat{\mathbf{n}}_\mathbf{i} \sim N(n(g_i), \sigma)$ is the heading of the pedestrian sampled from a distribution with the mean direction towards g_i and $v_p \sim N(V_p, \sigma_2)$ is the velocity of the pedestrian sampled from a mean pedestrian velocity V_p calculated from interactions with the goal, the environment and robot position.

The robot's own motion model follows from a velocity controller. In this paper we consider the robot to be constrained along a single lane. This simplifies the analysis without loss of generality in the discussion. $\mathbf{v}_r$ is the speed of the robot along the road.

$$\mathbf{x}_r{}' = \mathbf{x}_r + \mathbf{v}_r \Delta t + \epsilon_1$$
$$\mathbf{v}_r{}' = \mathbf{v}_r + \dot{\mathbf{v}}_r(a)\Delta t + \epsilon_2$$

where $\dot{\mathbf{v}}_r(a)$ denotes that the actual acceleration of the vehicle is influenced by the action taken in the previous step. The errors (ϵ_1, ϵ_2) are determined by the vehicle's controller characteristics.

The transition function $T_Y(x, g_i, a, x', g_i') : p(g_i'|g_i)$, shows the transition over the pedestrian intentions g_i. In general the pedestrian may change the intentions midway during execution and can be handled by our formulation. However in our analysis and results in this paper, we assume that during the course of the problem, pedestrian's intentions do not change. Interested readers are referred to [1] for a more general formulation of the problem of intention aware motion planning.

The focus of this paper is to formulate the problem of pedestrian avoidance as an intention aware motion planning problem and to show the effectiveness and feasibility of such an approach to autonomous navigation on the road. Once the problem is formulated as a MOMDP, any solver can be used to solve for the policy. In our case we use SARSOP [12], a leading point-based approximation algorithm, to solve our MOMDP model.

The corresponding MOMDP belief space is a union of lower dimensional belief subspaces over the goal set $\Theta : \{g_i\}$ at each observed state x.

$$\mathcal{B} = \bigcup_{x \in \mathcal{X}} \mathcal{B}_\Theta(x)$$

Here the dimensionality of the belief subspace $\mathcal{B}_\Theta$ is equal to the cardinality of the goal set Θ less 1, clearly reducing the computational complexity of the problem. The MOMDP value function is represented by a collection of alpha vector sets $\{\Gamma_\Theta(x) : x \in \mathcal{X}\}$.

$$V(x, b_\Theta) = \max_{\alpha \in \Gamma_\Theta(x)} \{\alpha \cdot b_\Theta\} \tag{1}$$

The belief is initialized to a uniform distribution over all goals. The online execution is performed in two steps: *action selection* and *belief update*. The action corresponding to the alpha vector that maximizes Eq.1 is chosen based on the current belief, b_Θ. The robot gathers observations resulting from its actions and updates the belief value (Eq.2) and the process repeats itself, until the robot reaches the goal.

$$b'_\Theta(g_i) = \eta T_Y(x, g_i, a, x', g_i') b_\Theta(g_i) \tag{2}$$

η being the normalizing constant.

Handling Multiple Pedestrians

A naive way of adding multiple pedestrians directly into the state space causes the problem to become intractable quickly. In addition since pedestrians are detected asynchronously, the time of detection has to be also incorporated further adding additional dimensions to the problem space. To avoid this we address each pedestrian independently. Once a pedestrian is detected, a new MOMDP problem is generated with uniform beliefs on the possible goals. This requires maintaining belief of each pedestrians according to Eq.2. Using the same policy, Π, different actions are chosen based on the unique belief state for each pedestrian. In general there can be many ways of combining these actions, we choose a simple conservative approach to pick the safest action based on a safety metric $S : \mathcal{X} \times A \rightarrow \Re^{+}$.

Let $\mathcal{M}_i$ denote the problem generated due to $\mathbf{p}_i$ and a_i denote the current action chosen for $\mathcal{M}_i$.

$$a = \arg\max_{i} \{S(a_i)\} \tag{3}$$

In general the safety metric can be defined on relative velocity or conservative lane changing or safety distance. In our campus environment the robot is constrained to move along a fixed lane, the only variability being controlling the speed. The safety metric we use is inversely mapped to the braking distance for the vehicle at the expected speed resulting from the decision and the speed controller.

3 Experiments and Results

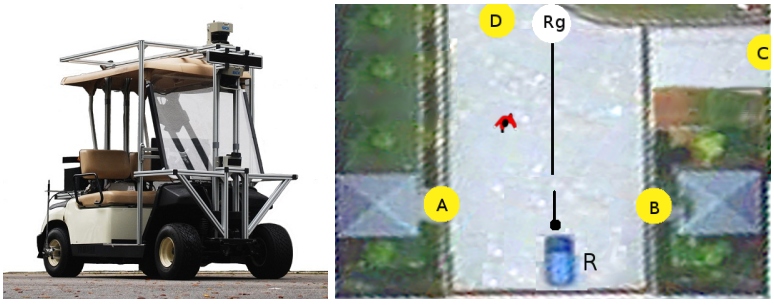

(a) Autonomous vehicle (b) Quadrangle environment

Fig. 3. Experimental Environments

We present the result of our intention aware pedestrian avoidance approach on the autonomous vehicle. Our autonomous system is a Yamaha golf-cart with drive by wire capability. Two onboard computers running ROS [16] on

intel i5 processors with 8Gb RAM execute various perception, planning and control algorithms. The vehicle is programmed to run at a maximum speed of 2m/s autonomously in a section of the NUS campus and can seat upto 2 people (Fig.3a). The vehicle is equipped with 3 LIDARs and a webcam. The LIDARs are used for localization while the combination of LIDAR and camera data is processed to identify pedestrians. More details about the system and its architecture is presented in [3].

3.1 Qualitative Comparison

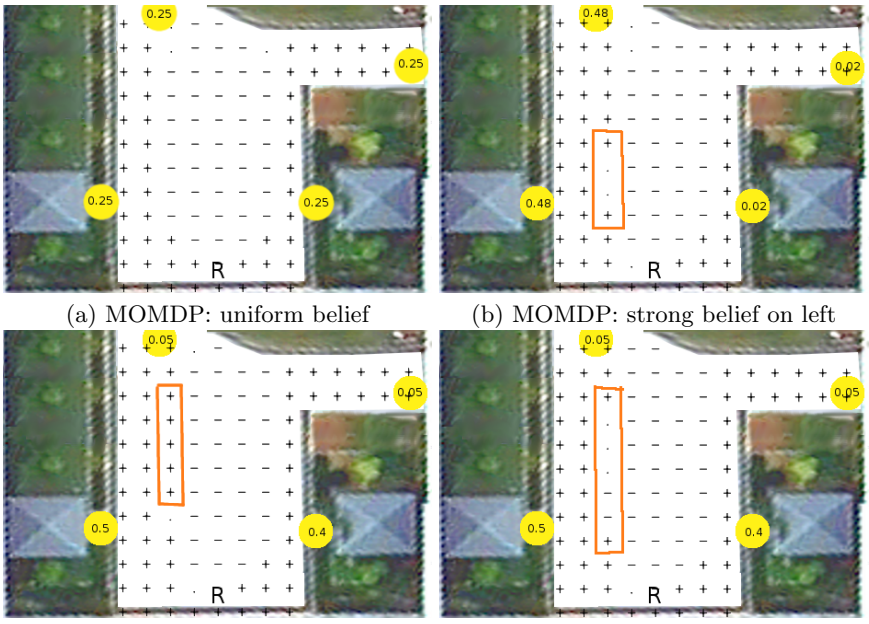

(a) MOMDP: uniform belief (b) MOMDP: strong belief on left

(c) Fixed belief: Bayes-ML (d) Fixed belief: MOMDP

Fig. 4. Comparison

Fig.3b shows the quadrangle in the engineering faculty of NUS where the students enter through (C & D). (A & B) are entrances to a shaded study area. Let us analyze the policy generated for this environment. Fig.4 plots the decision executed by the robot at R moving forward with velocity 1m/s for various positions of the pedestrians for a particular belief value over goals (displayed on the goal regions). The '+' sign represents the decision to accelerate when a pedestrian is present at that particular location, a '-' sign deceleration and '.' represents a decision to cruise accordingly. Fig.4(a & b) compares the spatial distribution of decision when the belief value over goals changes from uniform to being higher on left (goals, A & D). As the robot

becomes more confident about the pedestrian's intention, it's decisions are no longer overly conservative as shown by an increase in '+', helping it to navigate a more crowded environment. Note however that at locations where pedestrians stepping into the robot's path would require the robot to execute emergency avoidance, (marked by red box in Fig.4b) the robot's decisions are more cautious maintaining speed ('.') rather than accelerating ('+'). Note however that the lowest decision in the marked area is to accelerate. A quick calculation of the location and relative speed shows that by accelerating, the robot can overtake the pedestrian in case it tries to move towards B and hence is a safe decision.

Algorithm	Time (s): Mean (S.D)	Accident (4500 runs)
Bayes-ML	9.4 (6.4)	4.4 %
IA-MOMDP	9.6 (6.5)	3.4 %

Fig. 5. Performance comparison in simulation runs in quadrangle environment.

We next compare the result of a simple maximum likelihood (Bayes-ML) approach where the robot first picks the most likely goal and subsequently chooses an action based on the MDP policy learnt for that particular goal. We first look at a case in Fig.4c where the prediction on goals A and B are both high A being marginally higher. Since Bayes-ML does not take B into consideration, it ignores, as shown by '.' decision, the pedestrians at positions marked by red box. However, there is a significant chance of pedestrian at this location to go towards B. The MOMDP policy taking into account this possibility leads to a more conservative decision for the region under the same belief. To test how effectively does such a policy fare against Bayes-ML, we ran around 4500 simulations for pedestrians starting from random locations assigned to random goals. The results are shown in Table.5. We see that for similar time taken by the robot the MOMDP policy encounters significantly lower simulated collision states.

3.2 Perception Accuracy

Pedestrians are detected using a single webcam calibrated and mounted on top of a SickLMS 200 in front of the autonomous vehicle. The range data from the laser is clustered based on spatial proximity and a HoG person classifier [5] is run through the corresponding sub-image to label the cluster as a pedestrian or non-pedestrian [3]. Once sufficient confidence is reached that a cluster belongs to a pedestrian, a proximity based nearest neighbor data association is applied to track the pedestrian. The laser system runs around 50Hz while the vision runs at 15Hz. We performed controlled experiments where a person stood at known locations and the pedestrian detector was initiated and the data recorded. The false negative rate from the vision system was 20% over the number of frames computed. However this only affects the initialization phase of pedestrian detection since, once detected the range

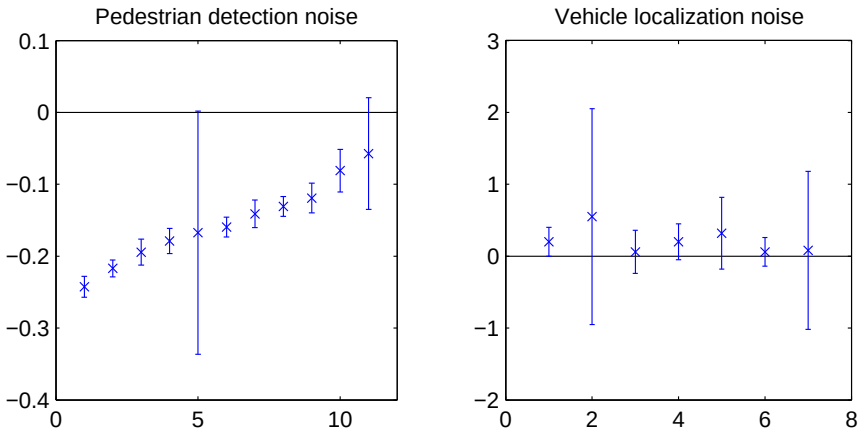

Fig. 6. Perception noise: the vertical axis shows error rate in meters, while horizontal axis marks the data point entries. The plots show that the noise is acceptable in assuming the pedestrian and vehicle positions as observed variables.

based data association is able to reliably track the pedestrian. On average it took around 0.46s to reliably detect the pedestrian. The mean distance error in detection is plotted in Fig.6a for various control positions of the pedestrian in order of increasing distance (5m to 25m at different angles) from the sensor. The error in distance estimate is under 30cm. The data point 5 was close a background wall (2m) which created a larger variation in the estimate error. Fig.6b shows the localization estimate of the vehicle following a simple curb based localization approach [15]. The error is under 1m which is quite acceptable to a vehicle of footprint 3m x 1.5m. Note also that the pedestrian is detected relative to the vehicle in the map. Thus the localization error only affects the uncertainty of the pedestrian's goal estimate and not the proximity estimate of the pedestrian w.r.t. the robot which is crucial for the pedestrian safety.

The results clearly validate the assumption of the MOMDP formulation where the only unobservable variable is the pedestrian's intentions, while the position of pedestrians and robot are sensed within acceptable accuracy.

3.3 Stationary Vehicle: Belief Tracking Experiment

In order to test the results of the MOMDP policy on a real system, we first kept the robot stationary at R in the quadrangle environment (Fig.3b), look at the decisions being made.

The snapshots in Fig.7(a & b), display the belief and the decision generated. A bar graph is plotted associated for each pedestrian, the left being the belief that the pedestrian is going to a goal to the left of the robot's heading

and the right correspondingly for the goals to the right. The red/green horizontal bar on the top denotes the decision made by the robot to STOP/GO w.r.t. the pedestrian.

The series of snapshots in Fig.7a, shows a couple of pedestrians (non-actors) walking in the quad. Each pedestrian is assigned a uniform belief upon detection. As more information is received the belief gets updated and the robot takes decisions accordingly. Note that the belief at snapshot (3-a) is higher over the goals (A & D) due to the stochasticity of the trajectory being followed. However, there is still a chance for him to move towards C. Taking this uncertainty into account, the decision of the robot is to STOP, which proves to be the right decision eventually.

While we formulate the problem for a single pedestrian, clearly a group of pedestrians moving cohesively generates exactly the same avoidance problem. Our cluster based approach tracks the belief over the group of pedestrians as would on a single pedestrian thereby avoiding the explosion of the problem space with additional pedestrians. The ability to quickly detect and generate a MOMDP avoidance problem makes the approach robust to splitting and merging over the clusters. Snapshots in Fig.7b show a group of pedestrians splitting to move to different goals. At snapshot (4-b) we see that the split is detected and a new problem generated and resolved for the left pedestrian.

The videos of all the runs and more experimental results are available at (*http://web.mit.edu/tirtha/Public*). We see that the pedestrian tracker is able to keep detect, instantiate and maintain the beliefs and decisions over various pedestrians. This is even robust to temporary occlusion, merging and splitting of people in the crowd.

3.4 Moving Vehicle: Pedestrian Crossing Experiment

We tested the algorithm on a real pedestrian crossing shown in Figure 8(a). The robot not only needs to detect the pedestrians and their intentions on the pedestrian crossing but also deal with jay walkers, a common phenomena in a campus environment. Figure 8(b) shows the robot interacting with such a pedestrian. The analysis is presented for a single pedestrian for clarity. The windows in clockwise direction from top left show the onboard camera view, the simplified environment representation used for solving the policy (the orange trajectory shows the pedestrian track in this environment and the green box shows the robot's position), the speed controller command velocity generated and the belief plots showing the evolution of the belief over pedestrian's goal as the pedestrian moves towards its intended goal. In the belief plot the color of the graph encodes the goal id.

Snapshots of the pedestrian at different times are merged into one camera window to show the development of the the belief. Notice that when the pedestrian is detected, the initial belief over the goals are equal. Due to high initial uncertainty the robot comes to a stop to wait for the pedestrian and collect more information about its intention. As the pedestrian starts moving

(a) belief tracking: cross (b) belief tracking: split

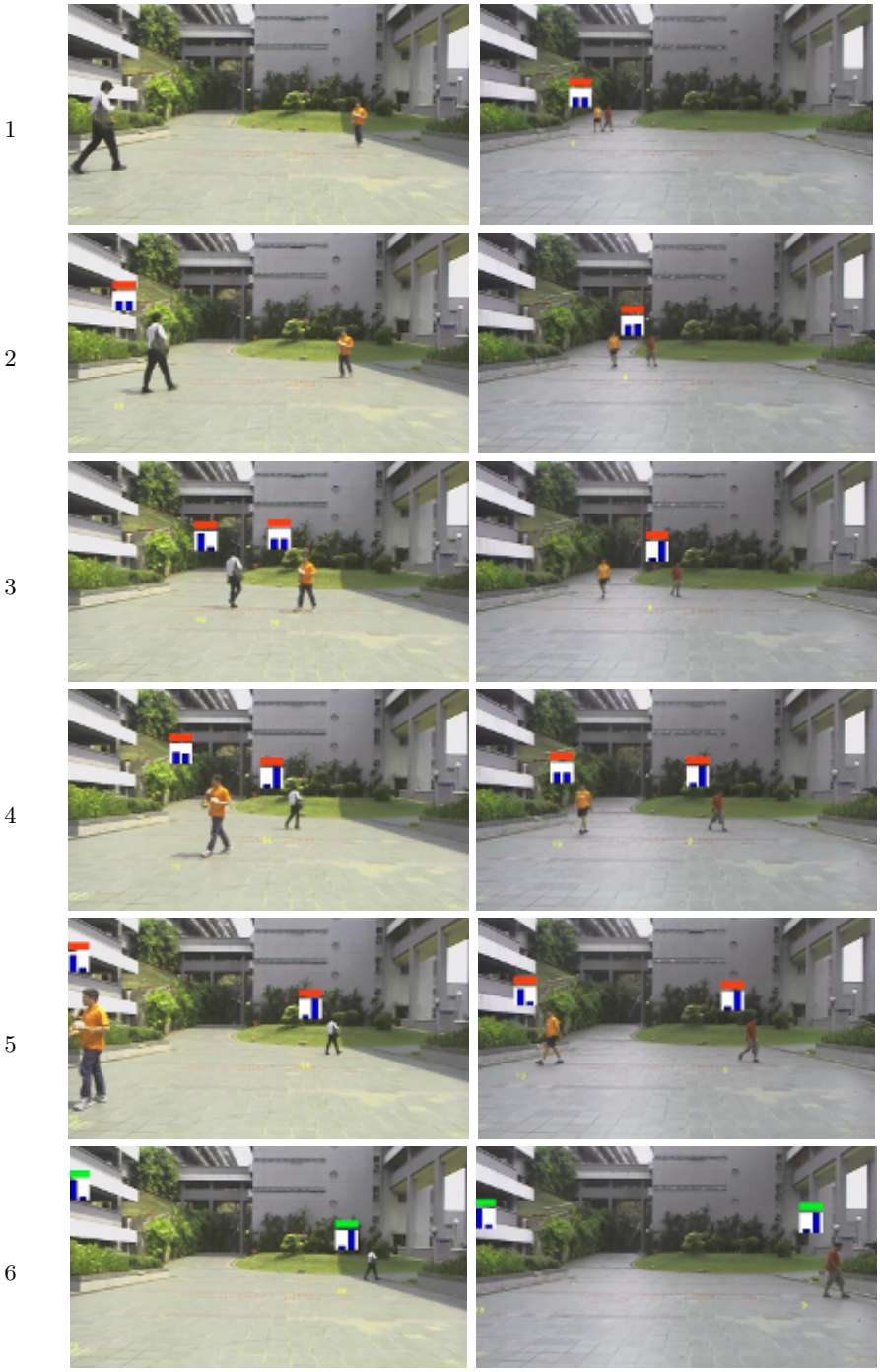

Fig. 7. Experimental Results (Best viewed in color).The videos of all the runs and more experiments are available at (*http://web.mit.edu/tirtha/Public*).

(a) A busy pedestrian crossing scene in the NUS campus that the vehicle has to navigate.

(b) Avoidance for a single pedestrian (on-board camera picture merged at different times to show the evolution of the belief)

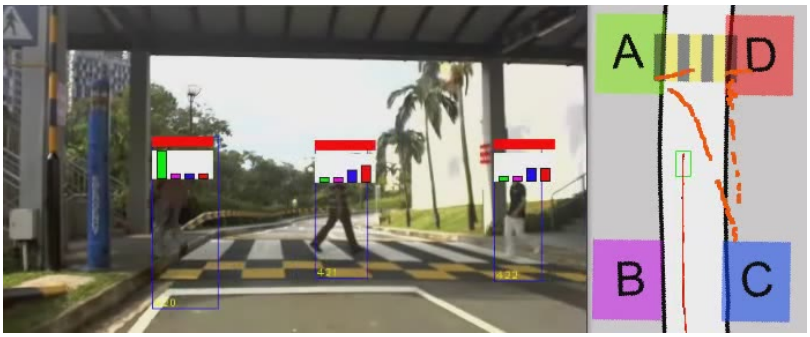

(c) Avoiding multiple pedestrians. (goals reordered and labeled differently than (b)). Each pedestrian generates a avoidance MOMDP and the beliefs are shown based on asynchronous set of observation history for each pedestrian.

Fig. 8. Pedestrian crossing experiment

across the road, the belief values over G2 and G1 increase while that of G0 and G3 drop as it is more likely that the pedestrian wants to move towards the other side. However there is a chance that the pedestrian will turn back and so the vehicle remains stationary. Slowly the belief over G1 grows stronger and that on G2 drops as the pedestrian starts moving diagonally. As soon as the belief over G1 is sufficiently large and the pedestrian is sufficiently out of the vehicle's path the vehicle starts moving. Figure 8(c) shows the vehicle responding to multiple pedestrians. Note that the goals are ordered and labeled differently however the environment setup and analysis is the same.

4 Conclusion

The paper presented an approach to avoid pedestrians on the road by identifying their intentions based on their actions on the road. We show in Sec.3.1, that trying to analyze the pedestrian's intentions helps in a better response to pedestrians than a naive distance based reactive approach (Fig.4(a&b)). Also maintaining the uncertainty over pedestrians goals gives a more conservative avoidance policy (Fig.4(c&d)) which leads to a lower simulated collision rates (Table.5). We also show that with proper factorization of the problem in terms of observed and unobserved variables, we reduce the computational complexity making it feasible to run the policy online on a realistic scenario. We demonstrated this on a vehicle interacting with multiple pedestrians in a real pedestrian crossing.

The main assumption in this work is the availability of pedestrian motion models and their finite intention models. An immediate extension of this work being addressed currently is to try to learn the intention models from the data collected and integrate it into the planning paradigm.

Even though the approach was presented for pedestrians on the road, such an approach could also be utilized to identify the intention of other human drivers on the road and could lead to a principled way of interacting safely with other drivers on the road.

References

1. T. Bandyopadhyay, K. S. Won, E. Frazzoli, D. Hsu, W. S. Lee, and D. Rus. Intention aware motion planning. In *Proceedings Workshop on Algorithmic Foundations of Robotics (WAFR)*, 2012.
2. R. Benenson, S. Petti, T. Fraichard, and M. Parent. Integrating perception and planning for autonomous navigation of urban vehicles. In *Proceedings International Conference on Intelligent Robots and Systems,*, pages 98 – 104, Beijing, Oct. 2006. IROS.

3. Z. J. Chong, B. Qin, T. Bandyopadhyay, T. Wongpiromsarn, E. S. Rankin, M. H. Ang Jr, E. Frazzoli, D. Rus, D. HSU, and B. K. H. Low. Autonomous personal vehicle for the first- and last-mile transportation services. In *Proceedings, International Conference on Cybernetics and Intelligent Systems and International Conference on Robotics, Automation and Mechatronics*, Qingdao, China, September 17-19 2011.
4. C. Coue, C. Pradalier, C. Laugier, T. Fraichard, and P. Bessiere. Bayesian occupancy filtering for multitarget tracking: An automotive application. *The International Journal of Robotics Research*, 25(1):19–30, January 2006.
5. N. Dalal and B. Triggs. Histograms of oriented gradients for human detection. In *CVPR*, pages 886–893, 2005.
6. D. Ellis, E. Sommerlade, and I. Reid. Modelling pedestrian trajectory patterns with gaussian processes. In *International Conference on Computer Vision Workshops*, pages 1229 – 1234, 2009.
7. R. Gayle, W. Moss, M. C. Lin, and D. Manocha. Multi-robot coordination using generalized social potential fields. In *International Conference on Robotics and Automation*, 2009.
8. D. Helbing, L. Buzna, A. Johansson, and T. Werner. Self-organized pedestrian crowd dynamics and design solutions: Experiments,simulations and design solutions. *Transportation Science*, vol. 39,(no. 1,):1–24, 2005.
9. P. Henry, C. Vollmer, B. Ferris, and D. Fox. Learning to navigate through crowded environments. In *Proceeding, International Conference on Robotics and Automation*, 2010.
10. R. Kelley, M. Nicolescu, A. Tavakkoli, M. Nicolescu, C. King, and G. Bebis. Understanding human intentions via hidden markov models in autonomous mobile robots. In *International Conference on Human Robot Interaction*, Amsterdam, Netherlands, March 1215 2008. IEEE.
11. O. Khatib. Real-time obstacle avoidance for manipulators and mobile robots. *Int. J. of Robotics Research*, 5(1):90–98, 1986.
12. H. Kurniawati, D. Hsu, and W. Lee. Sarsop: Efficient point-based pomdp planning by approximating optimally reachable belief spaces. In *Proceedings, Robotics: Science and Systems.*, 2008.
13. S. Ong, S. Png, D. Hsu, and W. Lee. Planning under uncertainty for robotic tasks with mixed observability. *International Journal of Robotics Research*, 29(8):1053–1068, 2010.
14. C. Papadimitriou and J. Tsisiklis. The complexity of Markov decision processes. *Mathematics of Operations Research*, 12(3):441–450, 1987.
15. B. Qin, Z. J. Chong, T. Bandyopadhyay, M. H. Ang, E. Frazzoli, and D. Rus. Curb-intersection feature based monte carlo localization on urban roads. In *To Appear Proc. Internation Conference on Robotics and Automation,*, 2012.
16. M. Quigley, B. Gerkey, K. Conley, J. Faust, T. Foote, J. Leibs, E. Berger, R. Wheeler, and A. Ng. Ros: an open-source robot operating system. In *Proceedings,International Conference on Robotics and Automation*, 2009.
17. D. Vasquez, T. Fraichard, and C. Laugier. Incremental learning of statistical motion patterns with growing hidden markov models. *Transactions on Intelligent Transportation Systems*, 10(3):403 – 416, Sept. 2009.